Secondary-Neutron-Yield Measurements by Current-Mode Detectors

Introduction

The measurement of secondary deuterium–tritium (DT) neutrons from pure-deuterium targets in inertial confinement fusion (ICF) experiments was proposed more than two decades ago[1–3] as a method for determining fuel areal density and demonstrated experimentally more than a decade ago.[4,5]

The secondary neutron yield is typically several orders of magnitude less than the primary yield, necessitating the use of a very sensitive neutron detector. For this application several single-hit detectors consisting of an array of individual scintillator detectors and electronics for detecting the time of flight of the first neutron (single hit) were developed at major laser facilities: LaNSA[6] at Nova, MEDUSA[7] at OMEGA, and MANDALA[8] at GEKKO. MEDUSA saturates on high-yield, direct-drive implosion experiments currently carried out on the 30-kJ, 60-beam OMEGA laser system and is not suitable for future cryogenic capsules experiments on OMEGA. At LLE we have developed several current-mode detectors (e.g., a single scintillator and a photomultiplier tube) for secondary-neutron-yield measurements on current and future OMEGA experiments. This article describes the status of these detectors, including detector design and calibration.

Comparison of Two Mode Detectors

For ICF experiments, single-hit detectors have many advantages (i.e., they are very sensitive and they can measure secondary neutron spectra and ion temperature in addition to secondary yield) but they also have two major disadvantages: First, single-hit detectors are very expensive because of the large number of individual detectors (~1000) and associated electronics. Second, they have a very limited dynamic range, which stems from the principle that an individual detector registers only the first hit. At low yield the single-hit detector is limited by statistical error simply from the number of fired individual detectors. To obtain less than 20% statistical error, 30 or more hits are necessary. If the number of fired individual detectors exceeds 50% of the array elements (500 detectors) at high yield, the single-hit detector is limited by a high number of double hits on a single detector. This effect can be compensated for to a certain extent by statistical analysis, but this so-called "busy correction" can extend the dynamic range by only a factor of 2. Consequently the dynamic range of the single-hit detector is 15 to 30 (with busy correction).

Current-mode detectors, e.g., a single scintillator and a photomultiplier tube connected with a digital oscilloscope, are much cheaper than single-hit detectors. The dynamic range of the current-mode detector is restricted by the linear dynamic range of the photomultiplier and can exceed 1000 for many photomultipliers. The operational range of the current-mode detector can be adjusted by changing location, the high voltage on the photomultiplier, or the scintillator. Since current-mode detectors are relatively cheap, it is possible to create several such detectors—each designed for a different secondary-yield range—and, thus, cover a large range of secondary yields without any change in setup. A disadvantage of the current-mode detectors is the fact that a very high secondary yield is required to measure energy spectra of secondary neutrons.

The dynamic range limitations of the single-hit detectors can be compensated for by modifying the targets—for example, by diluting the D_2 with H_2 or ^3He in the gas mixture to suppress the primary yield. We use such modifications for direct-drive ICF experiments with MEDUSA; however, this reduces the yield of secondary protons, which provide additional ρR information. A proton yield of 5×10^7 or higher, which is well beyond the MEDUSA range, is required to measure secondary proton spectra with a charged-particle spectrometer (CPS).[9] Target modifications are not possible for the cryogenic-target experiments planned on OMEGA, necessitating the development of current-mode detectors for secondary-yield measurements at LLE.

Background for Secondary Neutrons

Several background processes complicate the measurement of secondary neutrons:

1. *Hard x rays*. The hard-x-ray signal from laser–plasma interaction and from the peak compression can be very large

on OMEGA: x-ray energies can reach 500 keV.[10] As a result, the secondary neutron signal appears on the tail of the hard-x-ray signal. This complicates background subtraction for the secondary neutron signal. The hard-x-ray signal can be suppressed by lead shielding the scintillator counter.

2. *Neutron-induced gamma rays from the target chamber wall.* The primary neutrons interact with the target chamber wall and produce gamma rays, which are detected in the scintillator. This gamma-ray signal is several order of magnitudes smaller than the primary neutron signal but larger than the secondary neutron signal. It is practically impossible to suppress this gamma-ray signal by shielding because of its high energy. The timing of the gamma-ray signal depends on the size of the target chamber and the location of the scintillator counter and can be chosen to be before or after the secondary neutron signal.

3. *Neutron-induced gamma rays from the target and other structures.* The interaction of the primary neutrons with the target and other structures (target positioner, other diagnostics, etc.) within the target chamber creates gamma rays. For the current-mode detectors within the target chamber or close to it, these gamma rays may create background for the secondary neutron signal. The amount of background and its arrival time can be measured in ICF experiments that produce high yields with very low areal densities. There is no shielding against these gamma rays, but the location of the detector can be adjusted to move the gamma-ray signal away from the secondary neutron peak. For the current-mode detectors located far from the target chamber these gamma rays are not an issue since they fall between the hard x rays and the gamma rays from the target chamber wall.

Current-Mode Detectors at LLE

At the present time LLE has five current-mode detectors plus MEDUSA to measure secondary neutron yield. Historically, LLE's neutron bang time (NBT) detector was the first current-mode detector used to measure secondary neutron yield. The NBT detector is located inside the OMEGA target chamber in a 1.5-in. reentrant tube. The first NBT channel has a BC-422Q scintillator with 4826-mm^3 volume located 55 cm from the target chamber center (TCC) and a Hamamatsu H5783 photomultiplier connected to a 1.5-GHz LeCroy 9362 scope. The NBT detector is shielded from hard x rays by 1.5 in. of lead in front and 0.5 in. of lead surrounding it. LLE's NBT detector was not originally designed for secondary-yield measurements but has been calibrated against MEDUSA on several low-yield DT shots. An example of a scope trace of the

NBT detector for an indirect-drive DT shot with 3.4×10^7 yield is shown in Fig. 84.27. The DT peak on this scope trace was fit with a Gaussian function and is used for calibration. A scope trace of the NBT detector for a direct-drive DD shot with 8.0×10^{10} primary yield and 1.5×10^8 secondary yield is shown in Fig. 84.28. Figures 84.27 and 84.28 show that a lead thickness of 1.5 in. is not enough to shield from hard x rays on OMEGA. There are a few gamma-ray signals between the secondary-DT-neutron signal and the primary-DD-neutron signal. Because of the uncertainty in the gamma-ray background under the DT peak, the NBT error in the secondary neutron yield is estimated to be 20%. The NBT detector becomes nonlinear for secondary yields above 1.5×10^8, which was observed in comparison with other secondary-yield detectors described below. The NBT detector extends our measurable secondary yield beyond the MEDUSA range; it was used in comparison with the CPS diagnostic to measure secondary yield in direct-drive experiments. But recently another more
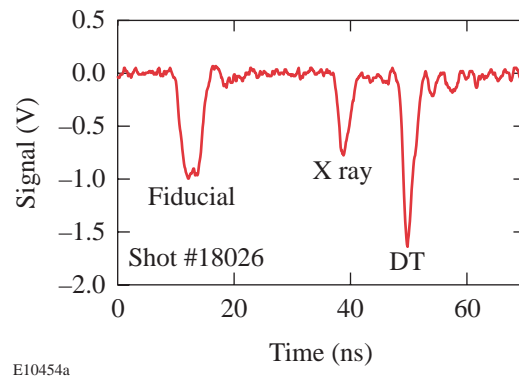

Figure 84.27
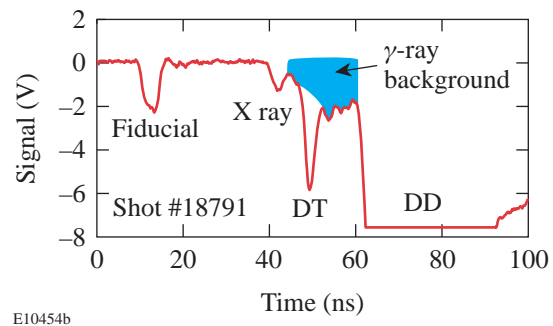Scope trace of the NBT detector signal on a DT shot with a 3.4×10^7 yield.

Figure 84.28
Scope trace of the NBT detector signal on a DD shot with a primary DD yield of 8.0×10^{10} and a secondary DT yield of 1.5×10^8.

precise and specially designed current-mode detector, 1.7MNTOF, replaced the NBT detector in secondary-neutron-yield measurements.

The other already existing scintillation counter that can be used as a current-mode detector to measure secondary neutron yield is the 3MLARD detector. It consists of a 17.78-cm-diam, 10-cm-thick scintillator coupled with an XP2020 photomultiplier connected to two channels of the Tektronix 684 scope. The 3MLARD detector is located 285 cm from the TCC and is shielded by a 0.75-in.-thick lead plate in front of the scintillator. An example of a scope trace for the direct-drive DD shot with 6.0×10^9 primary yield and 6.0×10^6 secondary yield is shown in Fig. 84.29. The signals from hard x rays, secondary DT neutrons, gamma rays from the target chamber wall, and primary DD neutrons (saturating the scope) are clearly seen. To measure secondary neutrons from the 3MLARD detector, the secondary neutron signal is integrated. We use in this detector a relatively low signal well below XP2020 saturation. The linearity of the 3MLARD was checked by comparison with other detectors. The 3MLARD detector was calibrated against MEDUSA for the secondary neutron yields; it does not extend MEDUSA's range but instead provides a second, independent measurement of the secondary neutron yield.

The 1.7MNTOF detector was designed specifically for measuring secondary neutron yield. It consists of a 40-mm-diam, 10-mm-thick fast BC 422Q scintillator coupled with a fast (250 ps) Photeck PMT240 microchannel-plate photomultiplier connected to two channels of a Tektronix 684 scope.

This detector is heavily shielded from hard x rays by 2 in. of lead in front and 1 in. of lead surrounding it. The 1.7MNTOF detector is located on the target chamber wall, 170 cm from the TCC. Because of its location, the 1.7MNTOF has no background from neutron-induced gamma rays from the target chamber wall. A scope trace of the 1.7MNTOF detector for a direct-drive DD shot with 8.5×10^{10} primary yield and 1.5×10^8 secondary yield is shown in Fig. 84.30. The signals from secondary DT neutrons and primary DD neutrons (saturating the scope) can be seen in Fig. 84.30. The hard-x-ray signal is completely eliminated by the lead shielding. From Fig. 84.30 one can estimate a gamma-ray background of a few percent. To measure secondary neutrons from the 1.7MNTOF detector we integrated the signal in the appropriate time window. The 1.7MNTOF detector was calibrated using ride-along copper activation on pure-DD shots; the result of this calibration is shown in Fig. 84.31. The copper activation is a standard diagnostic[11] for 14.1-MeV neutrons in ICF experiments with DT-filled targets. The ^{63}Cu $(n,2n)$ ^{62}Cu reaction cross section has a threshold at 10.9 MeV, and, therefore, copper activation is insensitive to the primary DD neutrons and registers only secondary DT neutrons. The secondary DT neutrons have an energy spectrum from 11.8 MeV to 17.1 MeV. The ^{63}Cu $(n, 2n)$ ^{62}Cu reaction cross section increases as the neutron energy increases.[12] We estimate the error from the uncertainty in the energy spectrum of the secondary neutrons to be less than 10%. This 1.7MNTOF calibration error can be improved if necessary by special low-yield DT calibration shots. The PMT240 photomultiplier is linear up to 25 V into a 50 Ω load. This level of signal has not yet been reached, and one can see from Fig. 84.31 that the 1.7MNTOF detector is linear over the range of yields measured. The PMT240 gain is 6×10^5 and the sensitivity of the 1.7MNTOF detector is about 0.3 pC/neutron.
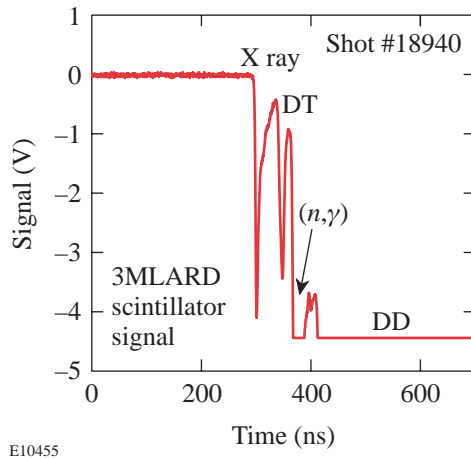

E10455

Figure 84.29
Scope trace of the 3MLARD detector signal on a DD shot with a primary DD yield of 6.0×10^9 and a secondary DT yield 6.0×10^6.
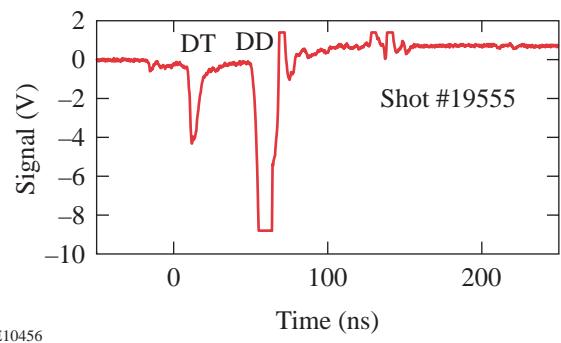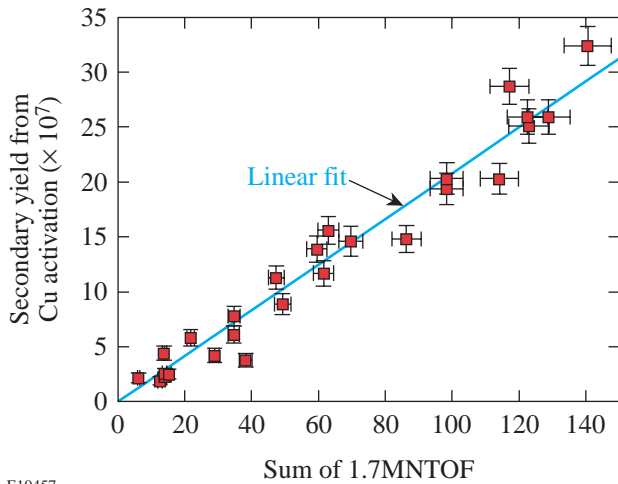

E10456

Figure 84.30
Scope trace of the 1.7MNTOF detector signal on a DD shot with a primary DD yield of 8.5×10^{10} and a secondary DT yield of 1.5×10^8.

The 20MLARD and 20M3×3 current-mode detectors are designed to extend the secondary-yield measurements to 5×10^{10}. The 20MLARD counter is identical to the 3MLARD counter. The 20M3×3 detector has a 3-in.-diam, 3-in.-thick scintillator and an XP2020 photomultiplier. Both detectors are located 20 m from the TCC behind the MEDUSA array and are shielded from hard x rays by 1.5-in. MEDUSA lead shielding and MEDUSA itself. Each of the detectors uses two channels of the Tektronix 2440 scope. A scope trace from the 20MLARD detector for the direct-drive DD shot with 1.0×10^{11} primary yield and 3.2×10^{8} secondary yield is shown in Fig. 84.32. The signals from hard x rays, gamma rays from the target chamber wall, secondary DT neutrons, and primary DD neutrons (saturating scope) along with small signals from the scattered neutrons can be seen in Fig. 84.32. A scope trace for the

20M3×3 detector looks very similar, but with lower signals. At this level of the secondary neutron yield there are just a few neutron hits in the 20MLARD and 20M3×3 current-mode detectors. We need higher yield for more precise calibration of these detectors. They can be calibrated with ride-along copper activation on moderate-yield DT shots. These two detectors will be used for the OMEGA cryogenic D_2 shots.[13]

The operating range of secondary yields of MEDUSA and all current-mode detectors at LLE together with the current status of the detectors is summarized in Table 84.IV. The lower limit of the yield range is determined by the neutron hit statistics, and the upper level is set by the measured or expected linearity threshold of the photomultiplier.

E10457

Figure 84.31
Calibration of the 1.7MNTOF detector against copper activation.
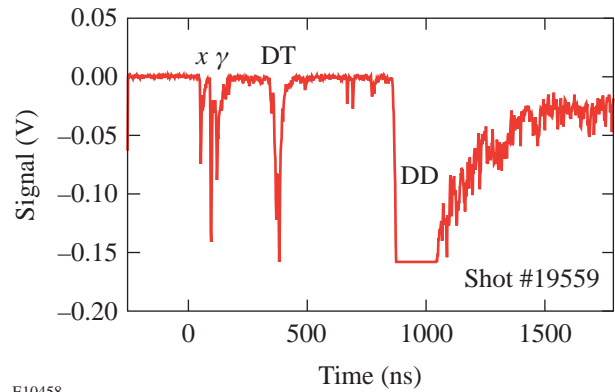
E10458

Figure 84.32
Scope trace of the 20MLARD detector signal on a DD shot with a primary DD yield of 1.0×10^{11} and a secondary DT yield of 3.2×10^{8}.

Table 84.IV: Detectors for secondary-yield measurements at LLE.

Detector	Yield Range	Current Status
MEDUSA	5.0×10^5 to 1.5×10^7	Calibrated
3MLARD	5.0×10^5 to 1.5×10^7	Calibrated
NBT	1.0×10^7 to 1.5×10^8	Calibrated
1.7MNTOF	1.0×10^7 to 1.0×10^9	Calibrated
20MLARD	2.0×10^8 to 5.0×10^9	Future calibration
20M3×3	5.0×10^8 to 5.0×10^{10}	Future calibration

Conclusions

Single-hit detectors like MEDUSA or LaNSA have a low dynamic range, which is inappropriate for the wide range of secondary yields obtained on OMEGA target shots. Current-mode detectors are an inexpensive alternative to single-hit detectors for measuring secondary neutrons over a wide range of yields. For the current direct-drive ICF experiments and future cryogenic experiments on OMEGA we have developed a set of current-mode detectors to measure secondary neutron yield from 5.0×10^5 to 5.0×10^{10} with an accuracy of 10%. The current-mode detectors have been used in several OMEGA direct-drive implosion experiments to measure secondary yield and will be used on future OMEGA cryogenic D_2 target shots.

REFERENCES

1. E. G. Gamalii *et al.*, JETP Lett. **21**, 70 (1975).

2. T. E. Blue and D. B. Harris, Nucl. Sci. Eng. **77**, 463 (1981).

3. T. E. Blue *et al.*, J. Appl. Phys. **54**, 615 (1983).

4. H. Azechi *et al.*, Appl. Phys. Lett. **49**, 555 (1986).

5. M. D. Cable *et al.*, Bull. Am. Phys. Soc. **31**, 1461 (1986).

6. M. B. Nelson and M. D. Cable, Rev. Sci. Instrum. **63**, 4874 (1992).

7. J. P. Knauer, R. L. Kremens, M. A. Russotto, and S. Tudman, Rev. Sci. Instrum. **66**, 926 (1995).

8. N. Izumi *et al.*, Rev. Sci. Instrum. **70**, 1221 (1999).

9. Laboratory for Laser Energetics LLE Review **83**, 130, NTIS document No. DOE/SF/19460-357 (2000). Copies may be obtained from the National Technical Information Service, Springfield, VA 22161.

10. C. Stoeckl, V. Yu. Glebov, D. D. Meyerhofer, W. Seka, B. Yaakobi, R. P. J. Town, and J. D. Zuegel, "Hard X-Ray Detectors for OMEGA and NIF," to be published in the Review of Scientific Instruments.

11. R. A. Lerche, W. R. McLerran, and G. R. Tripp, *Laser Program Annual Report-1976*, Lawrence Livermore National Laboratory, Livermore, CA, UCRL 50021-76, 3-105 (1976).

12. H. Liskien and A. Paulsen, J. Nucl. Energy **19**, 73 (1965).

13. R. L. McCrory, R. E. Bahr, T. R. Boehly, T. J. B. Collins, R. S. Craxton, J. A. Delettrez, W. R. Donaldson, R. Epstein, V. N. Goncharov, R. Q. Gram, D. R. Harding, P. A. Jaanimagi, R. L. Keck, J. P. Knauer, S. J. Loucks, F. J. Marshall, P. W. McKenty, D. D. Meyerhofer, S. F. B. Morse, O. V. Gotchev, P. B. Radha, S. P. Regan, W. Seka, S. Skupsky, V. A. Smalyuk, J. M. Soures, C. Stoeckl, R. P. J. Town, M. D. Wittman, B. Yaakobi, J. D. Zuegel, R. D. Petrasso, D. G. Hicks, and C. K. Li, in *Inertial Fusion Sciences and Applications 99*, edited by C. Labaune, W. J. Hogan, and K. A. Tanaka (Elsevier, Paris, 2000), pp. 43–53.